*Structural Engineering and Mechanics, Vol. 15, No. 3 (2003) 315-329*
DOI: http://dx.doi.org/10.12989/sem.2003.15.3.315


# Behaviour of interfacial layer along granular soil-structure interfaces

Wenxiong Huang†

*Discipline of Civil, Surveying & Environmental Engineering, School of Engineering, The University of Newcastle, NSW 2308, Australia*

Erich Bauer‡

*Institute of General Mechanics, Graz University of Technology, A-8010, Graz, Austria*

Scott W. Sloan‡†

*Discipline of Civil, Surveying & Environmental Engineering, School of Engineering, The University of Newcastle, NSW 2308, Australia*

*(Received September 10, 2002, Accepted January 24, 2003)*

**Abstract.** As shear occurs along a soil-structure interface, a localized zone with a thickness of several grain diameters will develop in soil along the interface, forming an interfacial layer. In this paper, the behaviour of a soil-structure interface is studied numerically by modelling the plane shear of a granular layer bounded by rigid plates. The mechanical behaviour of the granular material is described with a micro-polar hypoplastic continuum model. Numerical results are presented to show the development of shear localization along the interface for shearing under conditions of constant normal pressure and constant volume, respectively. Evolution of the resistance on the surface of the bounding plate is considered with respect to the influences of grain rotation.

**Key words:** soil-structure interface; shear localization; Cosserat continuum; hypoplasticity.

## 1. Introduction

Soil-structure interfaces are frequently met in geotechnical engineering. Shallow foundations, deep foundations, tunnels and earth retaining structures are examples with soil-structure interfaces. Compared with the interfaces between metals and rocks and other solid materials, the soil-structure interface has a more sophisticated behaviour. When shear occurs along a soil-structure interface, soil grains may rotate as well as slide along the structure wall. Intense shear deformation develops in a narrow zone of several grain sizes in soil along the interface, forming an interfacial layer. A high

† Postdoctoral Research Fellow
‡ Associate Professor
‡† Professor

gradient of heterogeneous deformation with pronounced shear dilatancy and grain rotations can be observed within the interfacial layer (Roscoe 1970, Brummund and Leonards 1973, Kishida and Uesugi 1987, Tejchman and Wu 1995). The mechanical properties of the granular material, the density and the stress state, the dilatancy resistance of the bounding structure and the roughness of the structure surface have a significant influence on the development of the interfacial layer, which in turn will affect the resistance of the system.

Soil-structure interface behaviour is mainly related to the phenomenon of shear localization in soil, which cannot be modeled properly within the framework of a classical continuum. Using classic continuum models, incipience of shear localization can be predicted via bifurcation analysis (Rudnicki and Rice 1975, Rice 1976). Due to the lack of a characteristic length on micro-scale, however, the post bifurcation behaviour is inaccurate and mesh sensitive (Needleman and Tvergaad 1984, de Borst *et al.* 1993, Huang 2000). To overcome this deficiency of the classic continuum approach, enhanced continuum theories have been used in recent years, including the micro-polar or Cosserat continuum approach (e.g., Mühlhaus and Vardoulakis 1987, de Borst 1991, Tejchman 1989), and the gradient-dependent continuum approach (e.g., Aifantis 1984, Vardoulakis and Aifantis 1989, de Borst and Mühlhaus 1992).

The present paper is focused on studying the behaviour of interfacial layers along granular soil-structure interfaces with a micro-polar continuum approach. The mechanical behaviour of granular soil is described using the framework of hypoplasticity (Kolymbas 2000). Micro-polar extensions of the hypoplastic models for non-polar continuum have been proposed for investigations of the problems related to shear localization (Tejchman 1994, 1997, Bauer and Tejchman 1995, Tejchman and Bauer 1996, Bauer and Huang 2001, Tejchman and Gudehus 2001, Huang *et al.* 2002). These models take into account the influence of granular rotation, shear dilatancy and contractancy for a wide range of pressure and density with a single set of constitutive constants, and offers the capability to capture the essential phenomenon of shear localization in granular materials. In the present work, the micro-polar hypoplastic model formulated by Huang *et al.* (2002) is used, which has the following advantages:

(1) Stationary states or the so-called critical states are consistently embedded in the constitutive model for the evolution of the stress tensor, the couple stress tensor and the void ratio. Under monotonic shearing the void ratio tends to the critical void ratio which is independent of the initial state. In contrast to the earlier versions the distribution of the void ratio is smooth within the localized zone and it does not exceed the critical void ratio;

(2) The limit stresses and the limit couple stresses are coupled in a rational manner, which allows a physical interpretation for the polar parameter;

(3) The thickness of the localized zone is scaled by a characteristic length which is proportional to the mean grain diameter and also related to the inter-granular friction.

The development of an interfacial layer along a granular soil-structure interface is studied by modelling the plane shear of an infinite granular layer located between two parallel rigid plates. In particular, the effects of the confining condition on the granular layer, surface roughness of the bounding plate and the influence of the polar parameter are investigated. Numerical results are presented for shearing of the granular layer under both constant normal pressure and constant volume.

## 2. Description of the model for cohesionless granular soil

This section presents a brief description of the micro-polar hypoplastic constitutive model for cohesionless granular materials. The hypoplastic concept by Kolymbas (1985) was originally proposed for a non-polar continuum and it is based on a non-linear tensor-valued function to model an inelastic material behaviour. Hypoplasticity can be understood as a generalization of hypoelasticity by Truesdell (1955). It differs from the concept of elastoplasticity in that neither a decomposition of the strain rate into an elastic part and a plastic part, nor the existence of a plastic potential, is assumed. A comparison between a hypoplastic model and an elastoplastic model can be found in Niemunis (1993) and Wu and Niemunis (1996). For basic information about hypoplasticity, readers can refer to Kolymbas (2000).

### *2.1 Outline of micro-polar continuum for plane strain problems*

A micro-polar continuum (Cosserat) is kinematically characterized by additional rotational degrees of freedom associated with each material particle, which is independent of particle translation (Schaefer 1967). For plane strain problems, each material particle has 3 degrees of freedom, that is, two translational degrees of freedom represented by $u_i$ ($i = 1, 2$) and one rotational degree of freedom denoted by $w_3^c$. The displacement component $u_i$ describes the macro-motion of a material particle and the Cosserat rotation $w_3^c$ describes its micro-motion (Eringen 1973). In the description of incremental mechanics, the deformation rate of such a micro-polar continuum is completely determined by the components $\dot{\varepsilon}_{ij}^c$ of the strain rate tensor and the components $\dot{\kappa}_{3j}$ of the micro-curvature rate tensor. These are defined as

$$\dot{\varepsilon}_{ij}^c = \dot{\varepsilon}_{ij} + \dot{\omega}_{ij} - \dot{\omega}_{ij}^c, \qquad \dot{\kappa}_{3j} = \dot{w}_{3,j}^c. \tag{1}$$

Herein $\dot{\varepsilon}_{ij} = (\dot{u}_{i,j} + \dot{u}_{j,i})/2$ are components of the strain rate tensor for a classical continuum, $\dot{\omega}_{ij} = (\dot{u}_{i,j} - \dot{u}_{j,i})/2$ are components of the spin tensor which represents the rigid body rotation or environmental rotation of a material element resulting from the macro-motion, and $\dot{\omega}_{ij}^c = e_{ij3}\dot{w}_3^c$ are components of the so-called Cosserat spin tensor, with $e_{ijk}$ being the permutation symbol. Corresponding to the spin tensor, an angular velocity for environmental rotation is determined by $\dot{w}_3 = -e_{3ij}\dot{\omega}_{ij}/2$. Generally, the strain rate tensor for the micro-polar continuum is non-symmetric. In the special case when the Cosserat rotation coincides with the environmental rotation, the symmetric strain rate for a classical continuum will be recovered.

Static quantities in work rate conjugation with the strain rates and the micro-curvature rates are the components of stress tensor $\sigma_{ij}$ and the couple stress tensor $\mu_{3j}$. With the couple stresses, the local equilibrium for a micro-polar continuum reads

$$\begin{aligned} \sigma_{ij,j} + b_i &= 0, \\ \mu_{3j,j} + e_{3ij}\sigma_{ij} + c_3 &= 0. \end{aligned} \tag{2}$$

Herein $b_i$ and $c_3$ represent components of the body force and the body couple, respectively. Note that due to the existence of couple stresses, the stress tensor is generally non-symmetric.

The equilibrium of a micro-polar continuum body with a volume $V$ can also be described in the weak form:

$$\int_V [(\sigma_{ij,j} + b)\dot{u}_i + (\mu_{3j,j} + e_{3ij}\sigma_{ij} + c_3)\dot{w}_3^c]dV = 0,$$

where the velocity components $\dot{u}_i$ and the Cosserat angular velocity $\dot{w}_3^c$ are independent of the static quantities. By applying Gaussian integration, the following equation can be obtained:

$$\int_V (\sigma_{ij}\dot{\varepsilon}_{ij} + \mu_{3j}\dot{\kappa}_{3j})dV = \int_V (b_i\dot{u}_i + c_3\dot{w}_3^c)dV + \int_S (t_i\dot{u}_i + m_3\dot{w}_3^c)dS, \tag{3}$$

where $t_i = \sigma_{ij}n_j$ and $m_3 = \mu_{3j}n_j$ are the surface traction components and the surface couple, respectively, and $n_j$ denotes the outward normal unit vector on the boundary surface $S$. With Eq. (3) the boundary conditions can be better understood. On boundaries of a micro-polar (Cosserat) continuum, either $t_i$ or $u_i$, and $m_3$ or $w_3^c$, must be prescribed.

### 2.2 Micro-polar hypoplastic model

The proposed micro-polar hypoplastic model (Huang *et al.* 2002), which is an extension of the hypoplastic model for a non-polar continuum developed by Gudehus (1996) and Bauer (1996), includes the stress tensor, the couple stress tensor and the void ratio as state variables. The evolution equations for the stress components, the couple stress components and the void ratio read:

$$\dot{\sigma}_{ij} = f_s[a_\sigma^2\dot{\varepsilon}_{ij}^c + (\hat{\sigma}_{kl}\dot{\varepsilon}_{kl}^c + \hat{\mu}_{3l}\dot{\kappa}_{3l}^*)\hat{\sigma}_{ij} + f_d(\hat{\sigma}_{ij} + \hat{\sigma}_{ij}^d)\sqrt{a_\sigma^2\dot{\varepsilon}_{kl}^c\dot{\varepsilon}_{kl}^c + a_\mu^2\dot{\kappa}_{3l}^*\dot{\kappa}_{3l}^*}], \tag{4}$$

$$\dot{\mu}_{3j} = d_{50}f_s[a_\mu^2\dot{\kappa}_{3j}^* + (\hat{\sigma}_{kl}\dot{\varepsilon}_{ij}^c + \hat{\mu}_{3l}\dot{\kappa}_{3l}^*)\hat{\mu}_{3j} + 2f_d\hat{\mu}_{3j}\sqrt{a_\sigma^2\dot{\varepsilon}_{kl}^c\dot{\varepsilon}_{kl}^c + a_\mu^2\dot{\kappa}_{3l}^*\dot{\kappa}_{3l}^*}], \tag{5}$$

$$\dot{e} = (1 + e)\dot{\varepsilon}_{kk}^c. \tag{6}$$

Herein $\hat{\sigma}_{ij} = \sigma_{ij}/\sigma_{kk}$ and $\hat{\mu}_{3j} = \mu_{3j}/(d_{50}\sigma_{kk})$ are components of the normalized stress and normalized couple stress, $\hat{\sigma}_{ij}^d = \hat{\sigma}_{ij} - \delta_{ij}/3$ are components of the deviator of the normalized stress, $d_{50}$ denotes the mean grain diameter (which enters the constitutive equations as an internal length) and $\dot{\kappa}_{3j}^* = d_{50}\dot{\kappa}_{3j}$. The summation convention for dummy indices is employed here. Note that in the special case of $\mu_{3j} = 0$ and $\dot{\kappa}_{3j} = 0$ or $d_{50} = 0$, the original hypoplastic relation by Gudehus (1996) and Bauer (1996), is recovered from Eq. (4).

The influence of the mean pressure $p = -\sigma_{kk}/3$ and the void ratio $e$ on the stress rate and the couple stress rate are taken into account by a stiffness factor $f_s$ and a density factor $f_d$:

$$f_s = \left(\frac{e_i}{e}\right)^\beta f_b, \quad f_d = \left(\frac{e - e_d}{e_d - e_d}\right)^\alpha, \tag{7}$$

where $f_b$ is a factor which can be derived from a consistency condition as shown by Gudehus (1996), and $e_i$, $e_c$ and $e_d$ represent the pressure-dependent maximum void ratio, critical void ratio and minimum void ratio, respectively. The following pressure-dependent relations, proposed for $e_i$ based on experiments by Bauer (1996) and assumed for $e_c$ and $e_d$ by Gudehus (1996), are adopted:

$$\frac{e_c}{e_{c0}} = \frac{e_d}{e_{d0}} = \frac{e_i}{e_{i0}} = \exp[-(3p/h_s)^n]. \tag{8}$$

Herein $\alpha$, $\beta$, $h_s$, $n$, $e_{i0}$, $e_{c0}$, and $e_{d0}$ together with the critical friction angle $\phi_c$, are constitutive constants which are also included in the non-polar hypopastic model of Gudehus and Bauer. The calibration of these constants can be carried out as discussed in detail by Bauer (1996) and Herle and Gudehus (1999).

The parameters $a_\sigma$ and $a_\mu$ in Eqs. (4) and (5) are related to the limit stress and the limit couple stress at stationary states. They are embedded in the current formulation in a different way to the earlier models by Tejchman and Bauer (1996), Tejchman (1997) and Bauer and Huang (2001), so that the void ratio does not exceed the critical void ratio at a stationary state. A stationary state is defined as the simultaneous vanishing of changes in stress, couple stress and void ratio while deformation is continuing. With the present model stationary states may be reached asymptotically in a localized zone for continuing monotonic shearing. It has been shown (Huang *et al.* 2002) that limit values of the state variables at a stationary state read

$$\hat{\sigma}^d_{ij} = \frac{-a^2_\sigma \dot{\varepsilon}^c_{ij}}{\sqrt{a^2_\sigma \dot{\varepsilon}^c_{kl}\dot{\varepsilon}^c_{kl} + a^2_\mu \dot{\kappa}^*_{3l}\dot{\kappa}^*_{3l}}}, \quad \hat{\mu}_{3j} = \frac{-a^2_\mu \dot{\kappa}^*_{3j}}{\sqrt{a^2_\sigma \dot{\varepsilon}^c_{kl}\dot{\varepsilon}^c_{kl} + a^2_\mu \dot{\kappa}^*_{3l}\dot{\kappa}^*_{3l}}}, \quad e = e_c. \tag{9}$$

Consequently, the limit stress and the limit couple stress at stationary states satisfy the following relation:

$$\frac{\hat{\sigma}^d_{ij}\hat{\sigma}^d_{ij}}{a^2_\sigma} + \frac{\hat{\mu}_{3j}\hat{\mu}_{3j}}{a^2_\mu} = 1. \tag{10}$$

Eq. (10) represents a super-ellipsoid surface in $(\hat{\sigma}^d_{ij}, \hat{\mu}_{3j})$ space, which indicates that a coupled limit condition is embedded in the model. It also provides an interpretation for the parameters $a_\sigma$ and $a_\mu$, i.e., $a_\sigma$ represents the magnitude of the deviator of the normalized limit stress in the case where the couple stress is zero (which is related to the internal inter-granular friction resistance against sliding), and $a_\mu$ represents the magnitude of the normalized limit couple stress at zero deviatoric stress (which is related to the internal inter-granular friction resistance against rotation). Numerical studies have shown (Huang *et al.* 2002) that the present constitutive model scales the thickness of the shear localization zones by a characteristic length factor

$$\delta = (a_\mu / a_\sigma) d_{50}, \tag{11}$$

which is proportional to the mean grain diameter and to the ratio $(a_\mu/a_\sigma)$. Parameter $a_\sigma$ depends on the critical friction angle of the granular material and the Lode angle in the deviatoric stress plane as discussed in detail by Bauer (2000). In this work, constant values are assumed for both $a_\sigma$ and $a_\mu$, with $a_\sigma$ being related to the critical friction angle $\phi_c$ according to

$$a_\sigma = \sqrt{\frac{8\sin^2\phi_c}{9(3+\sin^2\phi_c)}}. \tag{12}$$

## 3. Plane shear of an infinite sand layer

In this work, the shear behaviour along a soil-structure interface is studied numerically by simulating an infinite sand layer under plane shear (Fig. 1). The sand layer is modelled as a micro-polar hypoplastic continuum which is bounded by rigid plates. Due to the symmetry condition with respect to any vertical section, the field variables defined in the sand layer are independent of the horizontal coordinate $x_1$. Consequently we have $\dot{\varepsilon}_{11} = \dot{\varepsilon}_{33} = \dot{\kappa}_{31} = 0$, and the non-vanishing components of the strain rate and micro-curvature rate are:

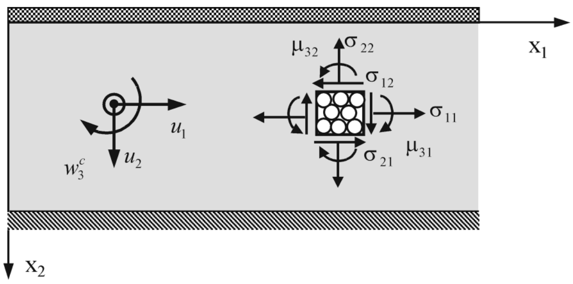


Fig. 1 Plane shear of a granular layer modelled as a micro-polar hypoplastic continuum

$$\dot{\varepsilon}_{22} = \frac{\partial \dot{u}_2}{\partial x_2}, \quad \dot{\varepsilon}_{12} = \frac{\partial \dot{u}_1}{\partial x_2} + \dot{w}_3^c = \dot{w}_3^c - 2\dot{w}_3, \quad \dot{\varepsilon}_{12} = -\dot{w}_3^c, \quad \dot{\kappa}_{32} = \frac{\partial \dot{w}_3^c}{\partial x_2}. \tag{13}$$

Herein $\dot{w}_3 = -\frac{1}{2}\partial \dot{u}_1 / \partial x_2$ represents the environmental angular velocity from macro motion.

By neglecting the body force and body couple, the equilibrium equations become

$$\frac{\partial \sigma_{12}}{\partial x_2} = 0, \quad \frac{\partial \sigma_{22}}{\partial x_2} = 0, \quad \frac{\partial \mu_{32}}{\partial x_2} - (\sigma_{12} - \sigma_{21}) = 0. \tag{14}$$

This means that the stress components $\sigma_{12}$ and $\sigma_{22}$ are constant across the granular layer, and the difference of the two shear stress components is related to the gradient of the couple stress on horizontal planes. For the following discussion, the granular layer is assumed initially to be in a homogeneous and isotropic state, i.e.,

$$\sigma_{ij}\big|_{(t=0)} = -p_0 \delta_{ij}, \qquad \mu_{3j}\big|_{(t=0)} = 0, \qquad e\big|_{(t=0)} = e_0. \tag{15}$$

Numerical calculations are performed for a medium dense granular layer with an initial void ratio $e_0 = 0.6$ and an initial pressure $p_0 = 100$ kPa.

Shearing is applied by moving the top layer of the granular body horizontally while fixing the bottom soil layer. Due to the additional degree of freedom on the boundary of the polar continuum body, boundary conditions for either Cosserat rotation or surface couple must be prescribed. In this study, Cosserat rotation on the top of the soil layer is prescribed following a modified form of the empirical relation proposed by Tejchman (1989). The Cosserat rotation is assumed to be proportional to the shear displacement normalized by the characteristic length $\delta$, rather than the mean grain diameter $d_{50}$, since the thickness of the localized zone is scaled by $\delta$ (see also the numerical results given in Fig. 7). Two special cases for shearing under different confining conditions are simulated, namely, constant normal pressure shear (CPS) and constant volume shear (CVS). The boundary conditions for CPS read:

$$x_2 = 0: \quad u_1 = u_{1T}, \quad \sigma_{22} = p_0, \quad w_3^c = f_w \frac{u_{1T}}{\delta},$$

$$x_2 = h: \quad u_1 = 0, \quad u_2 = 0, \quad w_3^c = \psi_0, \tag{17}$$

while the boundary conditions for CVS are:

$$x_2 = 0: \quad u_1 = u_{1T}, \quad u_2 = 0, \quad w_3^c = f_w \frac{u_{1T}}{\delta},$$

$$x_2 = h: \quad u_1 = 0, \quad u_2 = 0, \quad w_3^c = \psi_0. \tag{18}$$

Herein $h$ represents the thickness of the soil layer; $\delta$ is the characteristic length of the granular soil as defined in Eq. (11), $h \gg \delta$ is assumed so that the bottom boundary has little influence on the formation of an interfacial layer; and $\psi_0$ is a small value assigned for rotation to reduce the influence of the bottom boundary (which is more pronounced in constant volume shear).

The proportionality coefficient $f_w$ depends on the interaction between the grains and the bounding plate. Tejchman (1989) related $f_w$ to the relative roughness of the bounding surface, which is the roughness defined by Uesugi *et al.* (1988) divided by the mean grain diameter. In the authors opinion, such a relation needs further experimental verification to quantify the contributions of grain rotation and grain sliding to the relative displacement between the grains and the bounding plate (Bauer and Huang 2001). In the following, it will be assumed that a relative smoother bounding surface corresponds to a greater value for $f_w$. In the numerical calculations presented in this paper, different values are chosen for the coefficient $f_w$ to reflect the influence of the surface roughness of the bounding-plate. As the characteristic length $\delta$ is used to normalize the numerical results, $a_\mu / a_\sigma = 1$ is assumed in most calculations. Two exceptions, where $a_\mu / a_\sigma$ is set to 2.0 and 0.5, respectively, are used to show the influence of the polar parameter.

Other material constants used for the present calculations are those calibrated for Karlsruhe sand (Bauer 1996):

$h_s$ = 190 MPa, $n$ = 0.4, $\phi_c = 30^o$, $e_{i0}$ = 1.02, $e_{c0}$ = 0.82. $e_{d0}$ = 0.51, $\alpha$ = 0.14, $\beta$ = 1.05, $d_{50}$ = 0.5 mm.

## 4. Development of interfacial layer

In the following the development of an interfacial layer will be numerically investigated using the finite element method. The micro-polar hypoplastic model given in the previous section has been implemented into the program ABAQUS using a 4-noded isoparametric element with additional rotational degrees of freedom for plane strain problems (Hunag 2000, Huang and Bauer 2003).

Fig. 2 shows a contour plot of the void ratio from modelling of a CPS test for a prescribed horizontal shear displacement of $u_{1T} = h = 80\delta$ and for $f_w$ = 0.05 at the top of the layer. The profile of the displacement across the height of the layer indicates that the shear deformation is localized in a zone close to the moving top boundary forming an interfacial layer. The brighter area means

Fig. 2 Contour plot of void ratio obtained from a CPS test for $u_{1T} = h = 80\delta$ and $f_w$ = 0.05

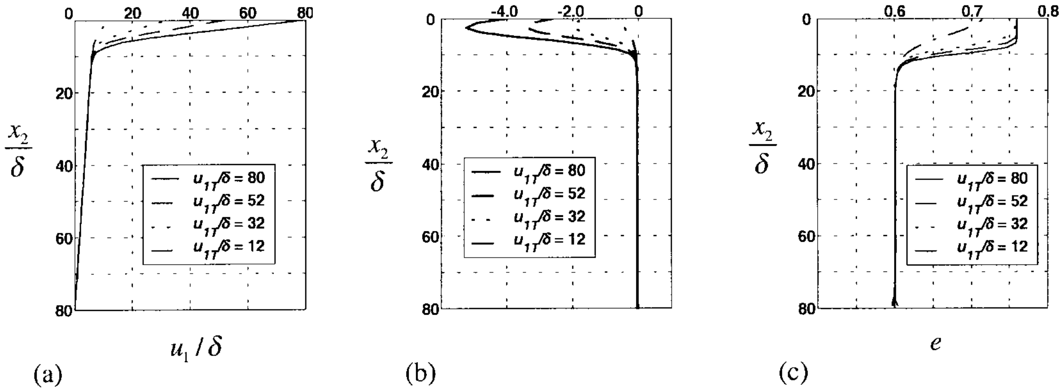


Fig. 3 Development of (a) horizontal displacement, (b) Cosserat rotation and (c) void ratio across the soil layer for constant normal pressure shear ($f_w$ = 0.05)

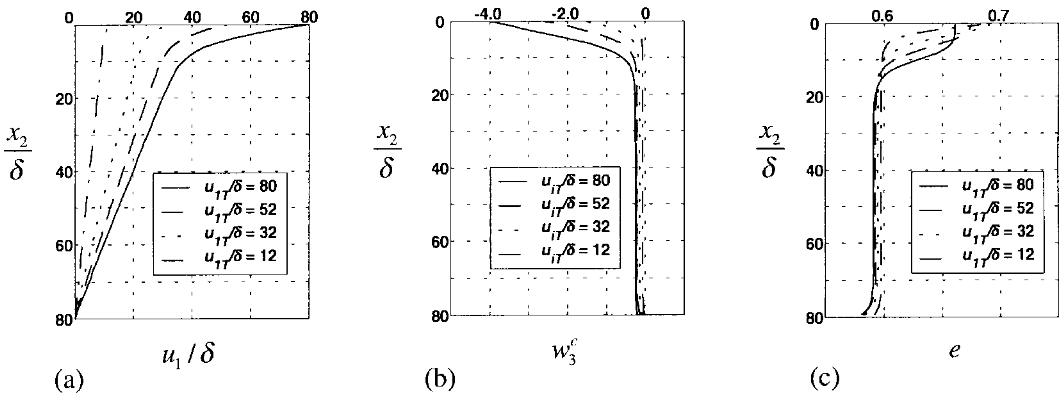


Fig. 4 Development of (a) horizontal displacement, (b) Cosserat rotation and (c) void ratio across the soil layer for constant volume shear ($f_w$ = 0.05)

higher void ratios as a result of dilation in the interfacial layer.

The development of the interfacial layer along the interface is shown in Fig. 3 for CPS and in Fig. 4 for CVS. During the first stage of shearing, deformation develops within the whole section of the soil layer, as indicated by the horizontal displacement. Further increase of shear displacement $u_{1T}$ causes localization. The additional horizontal displacement outside the interfacial layer is nearly zero (Fig. 3a for CPS), or develops much slower than that inside the interfacial layer (Fig. 4a for CVS). The thickness of the interfacial layer in this case is about 10 times the characteristic length $\delta$. Whether a shear test is conducted under constant normal pressure or constant volume condition has a strong influence on the displacement field, but has little influence on the thickness of the interfacial layer. Significant grain rotations, accompanied by dilatancy, are observed within the interfacial layer for both CPS (Figs. 3b, 3c) and CVS (Figs. 4b, 4c). This matches the experimental observations of Bogdanova-Bontcheva and Lippmann (1975), Löffelmann (1989) and Kashida and Uesugi (1987). As deformation localizes, Cosserat rotation almost stops developing outside the interfacial layer. For shearing under constant normal pressure, the volume of the soil body increases

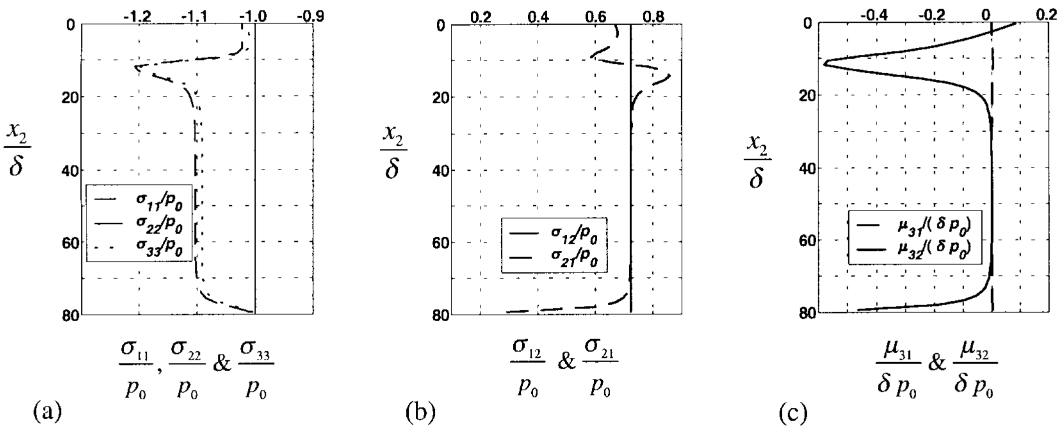

Fig. 5 Distribution of (a) normal stress components, (b) shear stress components and (c) couple stress components across the section corresponding to $u_{1T} = 80\delta$ (CPS, $f_w$ = 0.05)

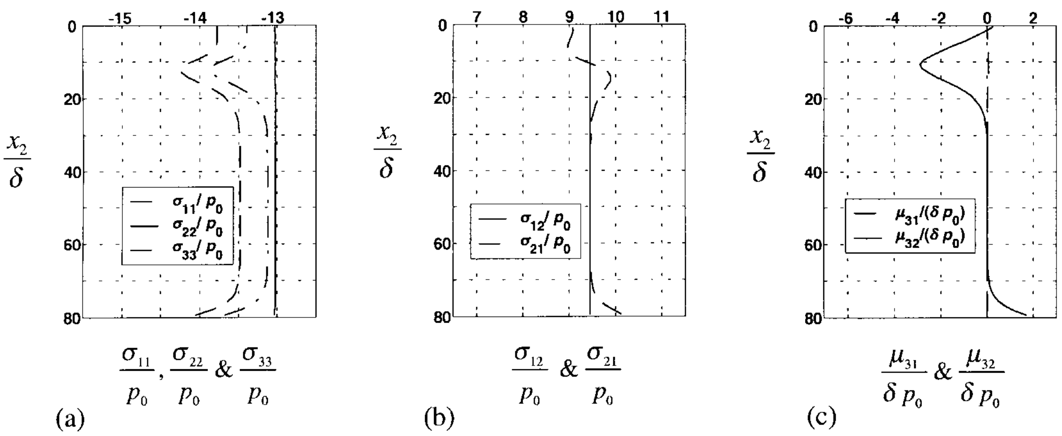

Fig. 6 Distribution of (a) normal stress components, (b) shear stress components and (c) couple stress components across the section corresponding to $u_{1T} = 80\delta$ (CVS, $f_w$ = 0.05)

as a result of pronounced dilation in the interfacial layer. However, for shearing under constant volume, dilation in the interfacial layer causes compression in the rest part of the granular body (see also Fig. 10b). Thus, the requirement for constant volume is globally fulfilled, i.e., the integral of the void ratio across the height of the shear layer remains constant.

The distribution of stress and couple stress components are shown in Fig. 5 for CPS and in Fig. 6 for CVS at a shear displacement of $u_{1T} = 80\delta$. The stress components $\sigma_{22}$ and $\sigma_{12}$ are constant as required by the equilibrium equations. The gradient of the couple stress $\mu_{32}$ is related to the difference of the shear stresses ($\sigma_{12} - \sigma_{21}$). The so called polar effect (Gudehus 1998) vanishes, except inside the localized zone and at the bottom where a boundary influence exists.

The influence of the polar parameter is shown by the numerical results given in Fig. 7 for CPS with $a_\mu / a_\sigma = 1.0$, 2.0 and 0.5, respectively. In these numerical calculations, the characteristic length $\delta$ is equal to 0.5 mm, 1.0 mm and 0.25 mm, correspondingly. The same finite element mesh is used and the same coefficient $f_w$ = 0.15 is assumed. This indicates a different normalized thickness of the

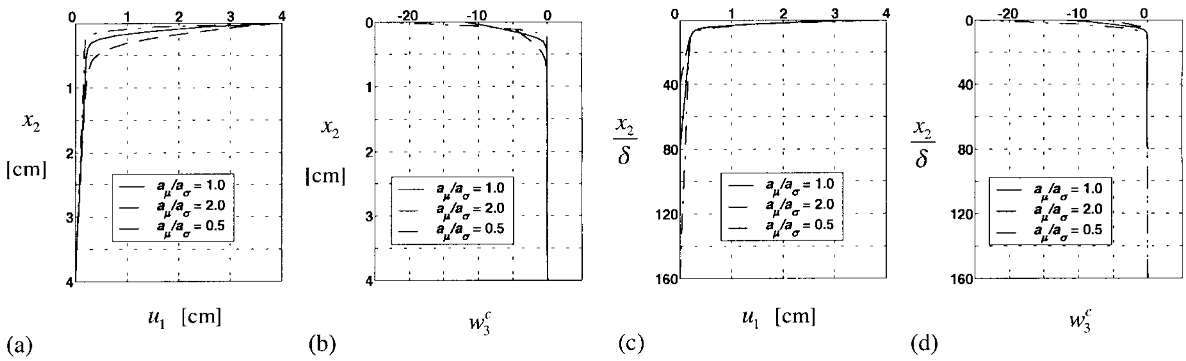


Fig. 7 Influence of polar parameter in constant normal pressure shear: Distribution of (a) & (c) horizontal displacement and (b) & (d) Cosserat rotation without and with normalization with the characteristic length $\delta$ ($f_w$ = 0.15)

sand layer and a different Cosserat rotation applied at the top of the sand layer with $w_3^c = 0.15u_{1T}/d_{50}$, $w_3^c = 0.15u_{1T}/(2d_{50})$, and $w_3^c = 0.15u_{1T}/(0.5d_{50})$, respectively. It can be seen from Figs. 7(a) and 7(b) that the thickness of the localized interfacial layer for the three cases is different, with a thicker interfacial layer arising for the smaller Cosserat rotation ($a_\mu/a_\sigma$ = 2.0) and a thinner interfacial layer arising for a larger Cosserat rotation ($a_\mu/a_\sigma$ = 0.5). However, the normalized thickness of the interfacial layer for these three cases is the same at large shear deformations (Figs. 7c and 7d).

## 5. Behaviour of the interfacial layer

The behaviour of the interfacial layer is explained with reference to Figs. 8-13.

In the calculations, the influence of the surface roughness of the top bounding plate is investigated by setting $f_w$ = 0.05, 0.15, and 0.40, respectively. Similar distributions of horizontal displacement, Cosserat rotation and void ratio are obtained for both CPS (Fig. 8) and CVS (Fig. 9), but with

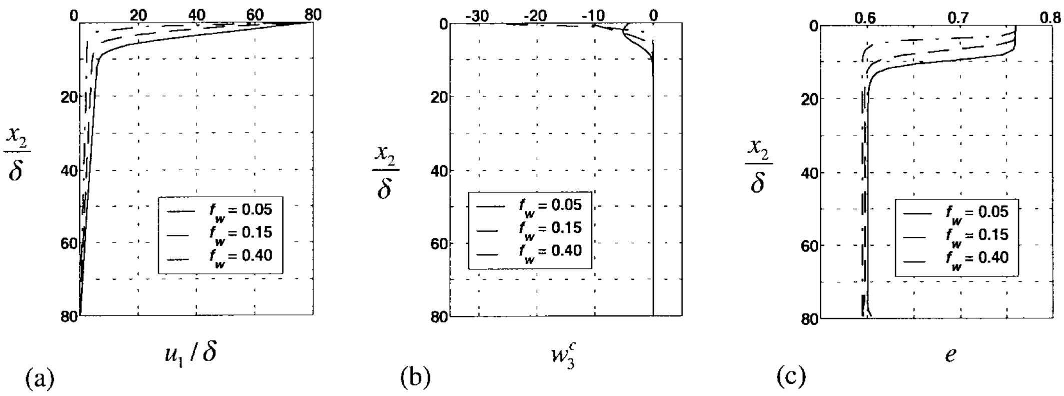


Fig. 8 Influence of coefficient $f_w$ in constant normal pressure shear: Distribution of (a) horizontal displacement, (b) Cosserat rotation and (c) void ratio across the soil layer

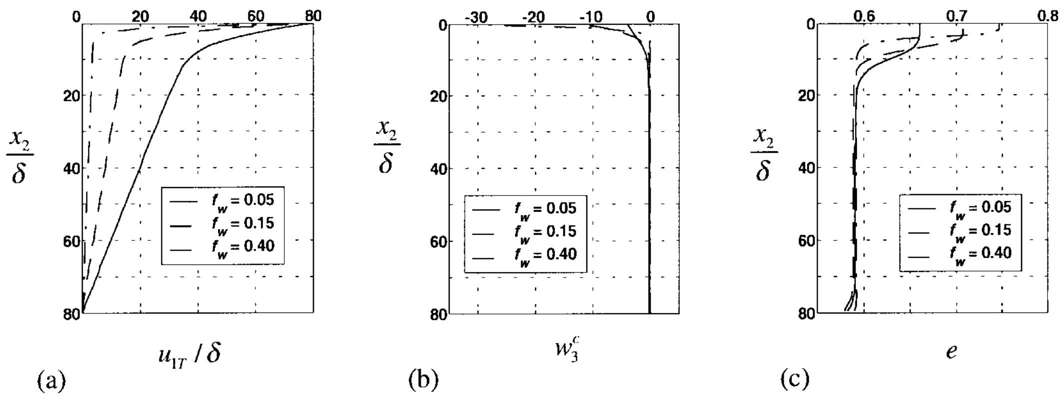


Fig. 9 Influence of coefficient $f_w$ in constant volume shear. Distribution of (a) horizontal displacement, (b) Cosserat rotation and (c) void ratio across the soil layer

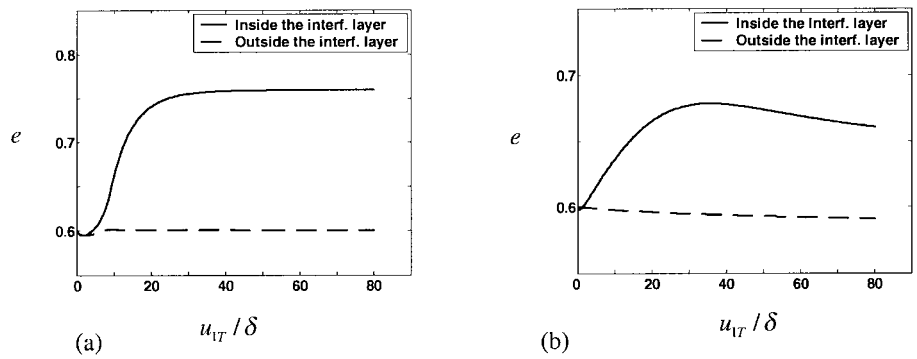


Fig. 10 Evolution of void ratio inside and outside the interfacial layer: (a) for CPS and (b) for CVS

different thicknesses for the interfacial layer where shear deformation localizes. With a greater value for $f_w$, which corresponds to a greater ratio of Cosserat rotation to normalized shear displacement along the interface (indicating a relatively smooth surface condition), a more significant localization with a thinner thickness occurs. Conversely, a smaller value for $f_w$, which corresponds to a relative rough surface condition, results in a less significant localization with a thicker thickness. However, the localized zone has almost the same thickness for CPS and CVS with the same $f_w$ as discussed in the foregoing section.

For shearing of a medium dense granular material shearing under constant pressure, the interfacial layer shows a pronounced dilation after an initial densification. The void ratio increases and then tends to a stationary value asymptotically under continued shearing (Fig. 10a). In contrast, the density of the granular material outside the interfacial layer ceases to vary after an initial increase. For shearing under constant volume, the void ratio inside the interfacial layer increases to a peak followed by a steady decrease, while the void ratio outside the interfacial layer decreases steadily from the earliest stage (Fig. 10b). The difference for the two cases may be attributed to the continuous increasing pressure in CVS resulting from localized dilation (see Fig. 12).

Fig. 11 and Fig. 12 show the evolution of the normal resistance $R_n = \sigma_{22}$ and the shear resistance

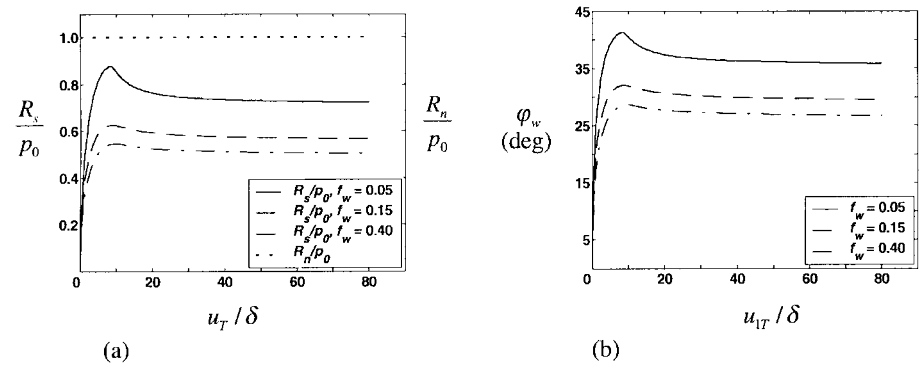


Fig. 11 Evolution of (a) shear resistance and normal resistance per unit area and (b) the wall friction angle on the interface for shearing under constant vertical pressure (CPS)

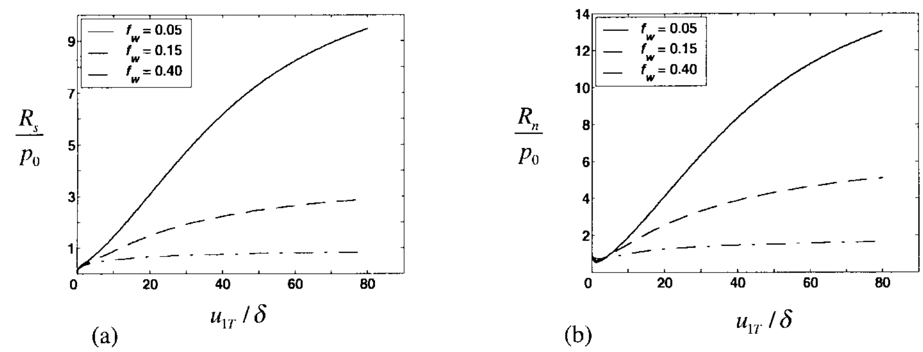


Fig. 12 Evolution of (a) shear resistance per unit area and (b) normal resistance per unit area on the interface under constant volume (CVS)

$R_s = \sigma_{12}$ normalized by the initial pressure $p_0$. For shearing under constant normal pressure, the shear resistance $R_s$ first increases steeply to a peak value and then decreases gradually to a stationary value while $R_n$ stays constant (Fig. 11a). The variation of frictional resistance of the bounding plate can be expressed by the stress ratio ($\sigma_{12}/\sigma_{22}$) or alternatively by the mobilized wall friction angle, $\varphi_w$, defined as

$$\varphi_w = \tan^{-1}(R_s/R_n) = \tan^{-1}(\sigma_{12}/\sigma_{22}). \tag{19}$$

As $R_n$ is constant in CPS, the evolution curves for the wall friction angle are similar to those for the bounding plate shear resistance. Two stages, characterized by a steep increase and then a gradual decrease can be distinguished (Fig. 11b). In response to a greater coefficient $f_w$, which corresponds to a greater grain rotation along the interface, a lower shear resistance (and a smaller mobilized friction angle) at peak and stationary states is obtained.

For shearing under the constant volume condition, both the normal and the shear resistance increase nonlinearly with increasing shear displacement (Fig. 12a). Within the range of shear displacement imposed, no limit value is reached for these resistances. It can be noted that the

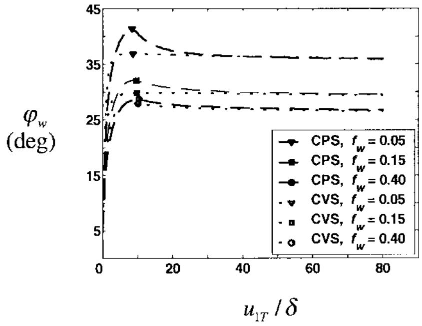


Fig. 13 Comparison of the wall friction angle for CPS and CVS

increase in normal resistance is due to dilation in the localized zone, which leads to an increase of shear resistance as a result of surface friction. The limit resistance will be achieved once the stationary state is reached in the localized zone. The coefficient $f_w$ has a strong influence on the magnitude of the resistances of the bounding plate against shearing. Greater normal and shear resistances are obtained for a smaller coefficient $f_w$. The wall friction angle $\varphi_w$, also shows a steeply increase phase, but followed by a very gradual decrease tending to a stationary value (Fig. 13, dotted curves). Like in shearing under constant normal pressure, the peak value and the stationary value of the wall friction angle decrease as $f_w$ is increased. Comparing the wall friction angles for CPS and CVS (Fig. 13), we see that, while more pronounced peaks are shown for CPS, the same stationary values are approached for the same coefficient $f_w$. This means that the peak values of the wall friction angle are influenced by the pressure developed in the granular layer, but the stationary values are independent of the pressure level. These results therefore also suggest that the influence of the surface roughness of the bounding plates can be pertinently reflected by the boundary condition using the relation between the Cosserat rotation and the shear displacement with the coefficient $f_w$, as assumed in Eqs. (17) and (18).

## 6. Conclusions

The development of an interfacial layer with a finite thickness along a granular soil-structure interface is caused by the formation of a zone in the granular soil where shear deformation localizes. With the proposed micro-polar hypoplastic model and suitably prescribed boundary conditions, the behaviour of a granular soil-structure interface is investigated by modelling plane shear of an infinite granular layer located between two parallel rigid plates under the conditions of constant normal pressure and constant volume.

When grain rotation develops along a bounding structure during shearing, deformation will be localized in the granular material in a narrow zone along the interface with pronounced dilatancy. An interfacial layer with the same thickness is obtained for shearing under either constant normal pressure or constant volume. The thickness of the interfacial layer is scaled by the size of the grains and it is strongly influenced by the interaction between the grains and the bounding structure. The rougher the surface of the bounding structure is, the thicker the interfacial layer will develop. When free dilation is allowed, as in the case of shearing under constant normal pressure, the shear resistance reaches a peak and then tends to a stationary value. When dilation in the granular material is confined, as in the case of shearing under constant volume, the shear resistance and the normal resistance increase continuously, without a recognizable peak. The evolution of the wall friction angle, however, shows a peak and tends to a stationary value for continuous shearing. The stationary value for the wall friction angle is influenced by the surface roughness of the bounding structure, but it is independent of how the bounding structure confines the granular body.

## References


Aifantis, E.C. (1984), "On the microstructural original of certain inelastic models", *J. Eng. Mat. Technol.*, **106**, 326-334.

Bauer, E. and Tejchman, J. (1995), "Numerical study of the effect of grain rotations and material behaviour in a fault zone", In Rossmanith (ed.) *Proc. 2nd Int. Conf. On Mechanics of Jointed and Faulted Rocks*. A.A. Balkema, 317-323.

Bauer, E. (1996), "Calibration of a comprehensive hypoplastic model for granular materials", *Soils and Foundations*, **36**(1), 13-26.

Bauer, E. (2000), "Conditions for embedding Casagrade's critical states into hypoplasticity", *Mech. Cohesive-Frict. Mater.*, **2**(2), 213-237.

Bauer, E. and Huang, W. (2001), "Evolution of polar quantities in a granular Cosserat material under shearing", In H.-B. Mühlhaus *et al*. (eds), *Bifurcation and Localisation Theory in Geomechanics*, Swets & Zeitlinger, Lisse, 227-238.

Bogdanova-Bontcheva, N. and Lippmann, H. (1975), "Rotationssymmetrisches ebenes Fliessen eines granularen Modellmaterials", *Acta Mechanica*, **21**, 93-113.

Brummund, W.F. and Leonards, G.A. (1973), "Experimental study of static and dynamic friction between sand and typical construction materials", *Journal of Testing & Evaluation*, **1**, 162-165.

de Borst, R. (1991), "Simulation of strain localization: A reappraisal of the Cosserat continuum", *Engineering Computations*, **8**, 317-332.

de Borst, R. and Mühlhau, H.B. (1992), "Gradient-dependent plasticity: formulation and algorithmic aspects", *Int. J. Numer. Method. Engng*., **35**, 521-539.

de Borst, R., Sluys, L.J., Mühlhaus, H.-B. and Pamin, J. (1993), "Fundamental issues in finite element analyses of localization of deformation", *Engng. Computations*, **10**, 99-121.

Eringen, C. (1976), "Polar and nonlocal field theories", *Continuum Physics*, Vol. IV. Academic Press, New York, San Francisco, London.

Gudehus, G. (1996), "A comprehensive constitutive equation for granular materials", *Soil and Foundations.* **36**(1), 1-12.

Gudehus, G. (1998), "Shear localization in simple grain skeleton with polar effect", In T. Adachi, F. Oka and A. Yashima (eds.), *Proc. 4th Int. Workshop on Localization and Bifurcation Theory for Soils and Rocks*, A.A. Balkema.

Herle, I. and Gudehus, G. (1999). "Determination of parameters of a hypoplastic constitutive model from properties of grain assemblies", *Mech. of Cohesive-Fric. Mater.*, **4**, 461-486.

Huang, W. (2000), "Hypoplastic modelling of shear localization in granular materials", PhD Thesis, Graz University of Technology.

Huang, W. and Bauer, E. (2003), "Numerical investigations of shear localization in a micro-polar hypoplastic materials", *Int. J. Numer. and Anal. Meth. Geomech.*, **27**, 325-352.

Huang, W., Nübel, K. and Bauer, E. (2002), "Polar extension of a hypoplastic model for granular materials with shear localization", *Mechanics of Materials*, **34**, 563-576.

Kishida, H. and Uesugi, M. (1987), "Tests of the interface between sand and steel in the simple shear apparatus", *Géotechnique*, **37**, 45-52.

Kolymbas, D. (1985), "A generalized hypoelastic constitutive law", *Proc. XI Int. Conf. Soil Mechanics and Foundation Engineering*, San Francisco, A.A. Balkema.

Kolymbas, D. (2000), *Introduction to Hypoplasticity*, A.A. Balkema.

Löffelmann, F. (1989), "Theoretische und experimentelle Untersuchungen zur Schüttgut-Wand-Wechselwirkung und zum Mischen und Entmischen von Granulaten", Doctoral thesis, University of Karlsruhe.

Mühlhaus, H.-B. and Vadoulakis, I. (1987), "The thickness of shear bands in granular materials", *Géotechnique*, **37**, 271-283.

Needleman, A. and Tvergaard, V. (1984), "Finite element analysis of localization in plasticity", In J.T. Oden and G.F. Carey (eds.), *Finite Elements: Special Problems in Soil Mechanics*, Prentice-Hall, 94-157.

Niemunis, A. (1993), "Hypoplasticity vs Elastoplasticity, Selected Topics", In D. Kolymbas (ed.) *Modern Approaches to Plasticity*, Elsevier, 277-307.

Oda, M., Konish, J. and Nemat-Nasser, S. (1982), "Experimental micromechanical evaluation of strength of granular materials: effect of particle rolling", *Mechanics of Materials*, **1**, 269-283.

Rice, J. (1976), "The localization of plastic deformation", In W.D. Koiter (ed), *Theoretical and Applied Mechanics*, North Holland Publishing Company, Amsterdam, 207-220.

Roscoe, K.H. (1970), "The influence of strains in soil mechanics, 10th Rankine lecture", *Géotechnique*, **20**(2), 129-170.

Rudnicki, J.W. and Rice, J. (1975), "Conditions for the localization of deformation in pressure sensitive dilatant materials", *J. Mech. Phys. Solids*, **23**, 371-394.

Schaefer, H. (1967), "Das Cosserat-Kontinuum", *Z. Angew. Math. Mech.*, **47**, 485-498.

Tejchman, J. (1989), "Scherzonenbildung und Verspannungseffekte in Granulaten unter Berücksichtigung von Korndrehungen", *Veröffentlichungen des Institutes für Bodenmechanik und Felsmechanik der Universität Fridericiana in Karlsruhe*, Heft 117.

Tejchman, J. (1994), "Numerical study on localized deformation in a Cosserat continuum", In R. Chambon, J. Desrues and I. Vardoulakis (eds.) *Localisation and Bifurcation Theory for Soils and Rocks*, A.A. Balkema, 257-274.

Tejchman, J. and Wu, W. (1995), "Experimental and numerical study of sand-steel interfaces", *Int. J. Numer. Anal. Meth. Geomech.*, **19**(3), 513-537.

Tejchman, J. and Bauer, E. (1996), "Numerical simulation of shear band formation with a polar hypoplastic constitutive model", *Computers and Geotechnics*, **19**(3), 221-244.

Tejchman, J. (1997), "Modelling of shear localisation and autogeneous dynamic effects in granular bodies", *Veröffentlichungen des Institutes für Bodenmechanik und Felsmechanik der Universität Fridericiana in Karlsruhe*, Heft 140.

Tejchman, J. and Gudehus, G. (2001), "Shearing of a narrow granular layer with polar quantities", *Int. J. Numer. Anal. Meth. Geomech.*, **25**, 1-28.

Truesdell, C. (1955), "Hypoelasticity", *J. Rat. Mech. Anal.*, **4**, 83-133.

Usugi, M., Kishida, H. and Tsubakihara, Y. (1988), "Behavior of sand particles in sand-steel friction", *Soils and Foundations*, **28**(1), 107-118.

Vardoulakis, I. and Aifantis, E.C. (1989), "Gradient dependent dilatancy and its implication in shear banding", *Ingenieur Archiv*, **59**, 197-208.

Wu, W. and Niemunis, A. (1996), "Failure criterion, flow rule and dissipation function derived from hypoplasticity", *Mech. of Cohesive-Frict. Mater.*, **1**, 145-163.